DEPARTMENT OF
GEOLOGY

Runoff, Infiltration, and Erosion Potential Along an Urban Headwater Stream

Andrew Simat

11/29/2023

GEOL 394

Advisor: Professor Prestegaard

Abstract:

Urban land uses and agricultural activities can add impervious surface cover or decrease infiltration rates, leading to erosive overland flow runoff. Hillslope and stream erosion resulting from this runoff can be extensive and it is a major reason for stream restoration activities. The need for restoration can be evaluated by examining processes that enhance erosion, such as runoff rate, and those that decrease erosion, such as high soil infiltration rates. This study was performed in an area of concern to residents of Greenbelt, Maryland. Measurements were made of soil properties (infiltration rate, bulk density, and soil organic carbon) that control soil permeability and water storage. The erosive power of overland flow during storm events has been determined from flow depth measurements obtained during storm events from 4 stream level loggers placed along the ephemeral stream. In the analysis, infiltration rates were measured in the topographic swale above the erosion feature. Measurements of flow depth, width, and area were measured at 4 locations along the channel after a major storm. Data indicates that infiltration rates in the swale above the head-cut are low, but that channel flow depth in the low gradient area is also low due to the width of the flow above the head-cut location. Stream water data loggers were installed in the field and relationships between rainfall amount and channel flow depth have been evaluated for data obtained from two separate storm events.

Introduction:

The motivation for this project came from Greenbelt residents who wanted to know whether expensive restoration activities were needed to keep the incised portion of a stream channel from cutting headward and creating a serious problem for the community (undermining roads, etc.) According to community residents, the head-cut has been at or near its current location for a while, but it is not clear why it is stable or if it will remain stable. To understand this question, I evaluated the effects of overland flow on erosion processes within a headwater stream in suburban Greenbelt, Maryland. The focus of the study is to investigate erosion processes in the tributaries below the storm sewer outfalls through the transition between an unchanneled swale (a shallow channel with sloping sides), and the head-cut of a deeply incised stream located in the densely wooded recreational area northeast of the community of Greenbelt. Measurement of channel flow depths and gradients, along with observations of erosion were used to determine erosional threshold levels in the actively eroding and non-incised portions of the stream. The incised channels are in headwater streams that receive runoff from suburban developments (Fig 1). Deeply incised parts of the stream are present at 2 locations: downstream of urban storm drains and downstream of a low gradient part of the stream.

The unchanneled swale above the main head-cut prevents direct connection between the incised headwater streams and the larger downstream head-cut. The development and maintenance of soil organic horizons might be important for water infiltration and storage due to local geology. The site is in a location where the clay horizon of the Potomac formation is close to the surface (Obermeier, 1984), which likely prevents deep infiltration of precipitation.

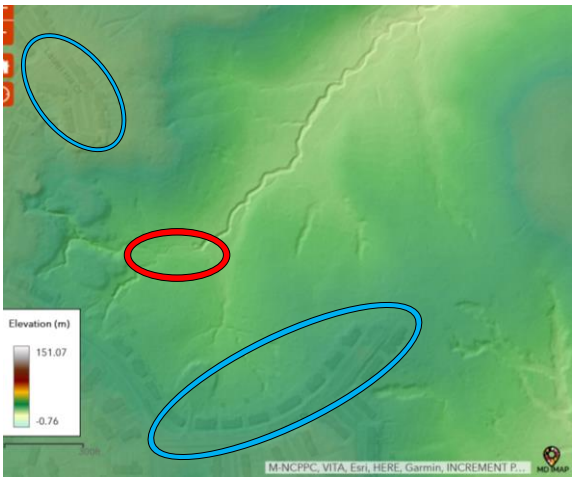

Fig 1. (Left) Map of part of Greenbelt, MD. Fig 2. (Right) Location of study encircled in red. Location of measurements encircled in red while urban development encircled in blue. Note the headwater tributaries that feed an unchanneled swale and an incised stream. (*ArcGIS Web Application*, n.d.)

Fig. 3. (Left) Photo of the swale above head-cut. Fig. 4. (Right) Photo from the head-cut looking upstream towards the swale. Photos by Greenbelt resident C. Plaisant.

Similar first order streams with large head-cuts located below unchanneled swales are found in other reforested regions of the Coastal Plain with similar underlying geology, and similar land-use histories (formerly agricultural), but most are in areas with no urban development. Examination of these sites indicate that: a) some of these forested stream channels are fed primarily by subsurface flow and are located downstream of headwater

wetlands, and b) evidence of upslope gully erosion, likely associated with previous agricultural activity is widespread. The gully form, however, is filling with leaves and sediment that are being transported in via winds and gravity. In addition to this, the gully form is filling in with organic matter and soil if they no longer receive agricultural or urban runoff. This is observed in Greenbelt National Park and recorded in the literature for other sites (Castillo and Gomez, 2016; Chen et al., 2013).

Runoff from upstream urban sites is typically higher than runoff from forested landscapes (MacDonald and Coe, 2007; Gregory et al., 2006; Rose and Peters, 2001; Leopold, 1968). Runoff from urban development with a relatively small footprint (in this case just the Greenbelt hill tops), may generate excess runoff that could be infiltrated into the forested hillslope and swale. This would more likely occur during low intensity storm events. Therefore, channel and swale infiltration rates could influence the amount of urban runoff that is carried across the swale to the main head-cut and enhance erosion at the major gully. In addition to this, the stream gradient could affect local erosion.

Background Information

Geology:

The town of Greenbelt is underlain by the Potomac Group, a Cretaceous-age formation that outcrops east of the Fall Zone in Maryland (Glaser, 2003). The Potomac Group consists of several different units. An upper sand and gravel unit is found under the tops of hills (Fig 5). This sand and gravel unit is underlain by sand and clay units. The clay units have low permeability and affect subsurface drainage and hillslope stability (Obermeier, 1984). Soils developed on the hillslopes are thick enough to support densely wooded forests while also maintaining low soil erosion rates (Chen et al., 2013).

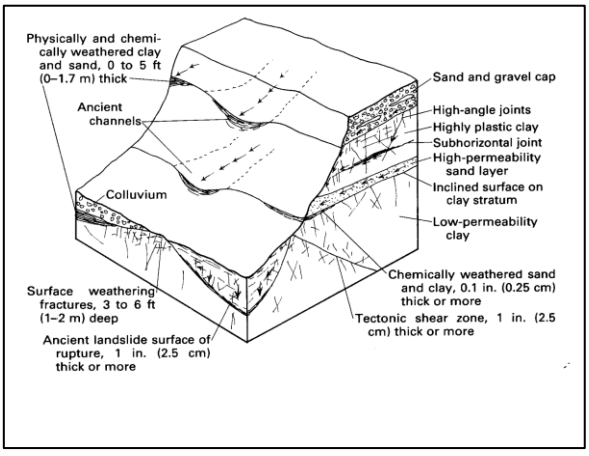

Fig 5: Stratigraphy of the Potomac Group, showing upper sand and gravel horizons and lower clay horizons. From Obermeier, 1984.

Channel Head Erosion:

Channel heads can form as water is delivered to the valley axis either by groundwater flow or by overland flow. Many headwater streams in forested sites in the Maryland Coastal Plain are in convergent headwater basins that likely originally contained headwater wetlands. In a reference site in Greenbelt National Park, a small channel formed downstream of the headwater wetland. The wetland formed in an area of low gradient, convergent region of the hillslope. The small channel in Greenbelt National Park is in a similar topographic position as the deep head-cut at the Greenbelt town study site.

Although both overland flow (from agricultural or urban areas) and saturated overland from wetlands or temporarily saturated areas can generate sufficient flow depth to erode channel heads, saturated overland flow usually requires greater upslope basin area (Montgomery and Dietrich, 1988) than runoff from urban areas to achieve critical flow depths to cause local erosion. Shear stress, calculated using the DuBoys equation, is expressed as (Schwendel et al., 2010):

$$\tau = \rho g d S$$

where τ = shear stress (dynes/cm^2, $\mathrm{N/m}^2$), ρ = water density (g/cm^3), g = gravitational acceleration (m/s^2), d = water depth (cm), and S = local gradient.

For overland flow to erode bare soil, critical shear stress values must be reached. These values vary with soil type, but previous studies indicate values of around 150 dynes/cm^2. In grassed areas, threshold shear stresses are 2,000 dynes/cm^2. Forested regions usually do not support dense grasses, and groundcover, such as the English Ivy present in the surrounding research area, provides poor resistance to soil erosion (similar to bare soils). Therefore, shear stresses greater than 150 dynes/cm^2 might be reached in areas where overland flow is on steep slopes, the flow depth is deep, or there is a critical combination of depth and gradient.

Stream Longitudinal Profile and Stream Gradient:

As a replicable reference data set, Dr. Prestegaard constructed a stream longitudinal profile (Fig 6) and a stream gradient graph using data from the ArcGIS Web Application (Fig 7). They indicate the steep incised tributaries, the low gradient swale, and the incised head-cut. These topographic data are not sufficient to determine gradients in the low gradient swale between the tributary junction and the head-cut, therefore, regions from the lower tributaries to the head-cut have been surveyed with surveying equipment (usually 0.5 cm vertical resolution). This survey occurred on 4/24/23 and includes surveying in the elevations of the gully water level records. Collected data from the survey are displayed in Appendix C. The longitudinal profile and stream gradient of the main tributary, the axis of the swale, and

downstream channel are shown in Fig 6. This profile is based on the Maryland lidar data with 10 cm vertical resolution. Fig 6 represents the tributary long profile, plotted as distance (in km) versus elevation (in m). Fig 7 shows the local gradient (m/m) as a function of distance downstream.

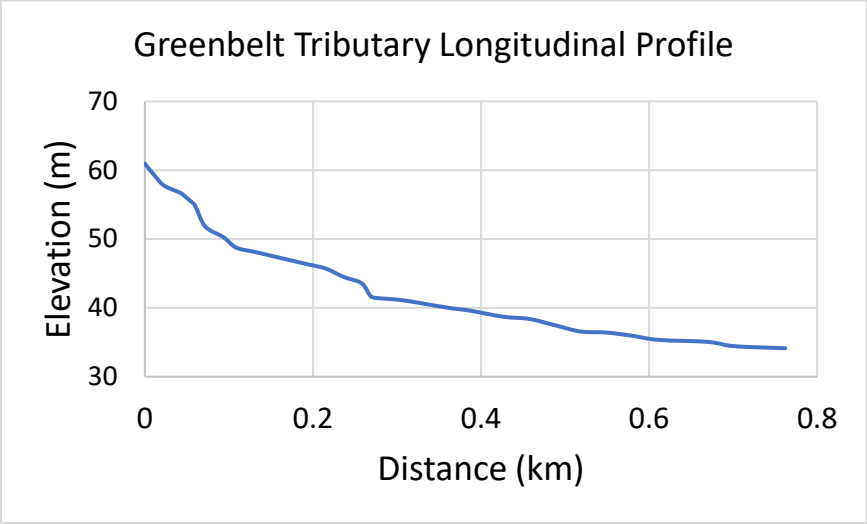

Fig 6. Local Greenbelt Longitudinal Profile

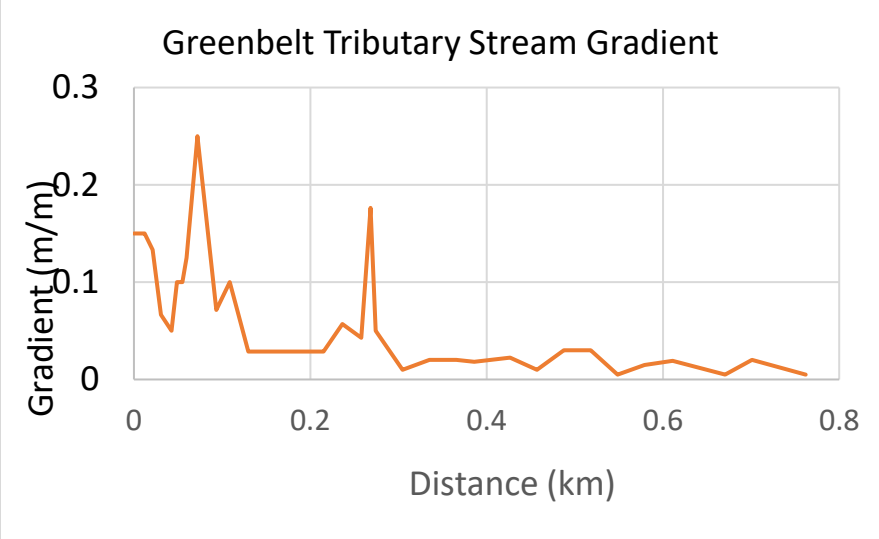

Fig 7. Local Greenbelt Stream Gradient Profile

Hypotheses:

HY1: Urban runoff delivered at sewer outfalls is leading to active stream channel erosion further downstream.

Null hypothesis: Stormwater runoff has little impact on stream channel erosion further downstream.

HY2: Stream water infiltration and/or energy dispersion reduces the impact of stormwater downstream from initial sewer outfalls.

Null Hypothesis: There is no observable stream channel infiltration and/or energy dispersion downstream from initial sewer outfalls.

Methods:

To test these hypotheses, I conducted the following analyses: a) measure soil properties: infiltration capacity, soil bulk density, and organic matter content along stream axis sites that receive urban runoff, b) survey elevations along the channel to determine local stream gradient along the stream profile, c) obtain local precipitation data from a nearby precipitation gauge, d) measure peak flow depth at locations along the urban runoff channel for bank-full conditions and during storm events using data loggers, e) develop relationships between precipitation and channel flow depth for each site, and f) use stream gradient and channel flow depth to determine channel shear stress for measured storm events and compare with critical shear stresses to erode bare or vegetated surfaces.

The project began by measuring soil infiltration rates at multiple sites within and outside the valley axis above the stream incisions of interest. Soil samples were taken and organic horizon depth, and soil bulk density data were determined near sites of infiltration measurements. Streamflow depth along the stream axis has been determined by installing stream water recorders at 4 points along the stream to determine: 1) the size of the storm event required to initiate overland flow runoff, 2) flow depth at locations along the stream profile, and 3) the local shear stress for each of these storm events. The project examined connections among local soil infiltration rates, soil organic matter and soil bulk density in relation to soil erosion (Fanelli et al., 2017; Wynn et al., 2004).

Soil Properties:

Three soil cores/properties were measured at the field site or in the lab. Soil infiltration capacity was measured in the field using installed falling head infiltrometers. Soil cores for bulk density and soil organic matter (SOM) analyses have been taken from Greenbelt along the urban stream profile, particularly in the unchanneled areas above the head-cut. Soil cores were taken at similar topographic positions at reference sites that are along stream axes but do not receive urban runoff. Core samples have been taken of the O (organic) horizon, and the upper A horizon. These samples were weighed, dried, and reweighed to determine initial moisture content and bulk density.

Bulk density is the weight of the soil per unit volume. Soil cores of known volume were weighed, dried in an oven at 60°C for 8-12 hours, and reweighed. From these measurements, soil moisture (wet-dry weight)/volume and soil dry bulk density was determined. Soil organic matter was estimated from previously determined relationships between bulk density and organic matter. Said previous measurements were made using loss on ignition for similarly aged forests on similar geological materials (Volz et al., 2022; Volz 2020).

Peak Flow Depth During Storms:

Four stream water level and temperature loggers (Hobo) were installed in the incised tributary channels below the tributary junction at the head of the swale (Fig 8).

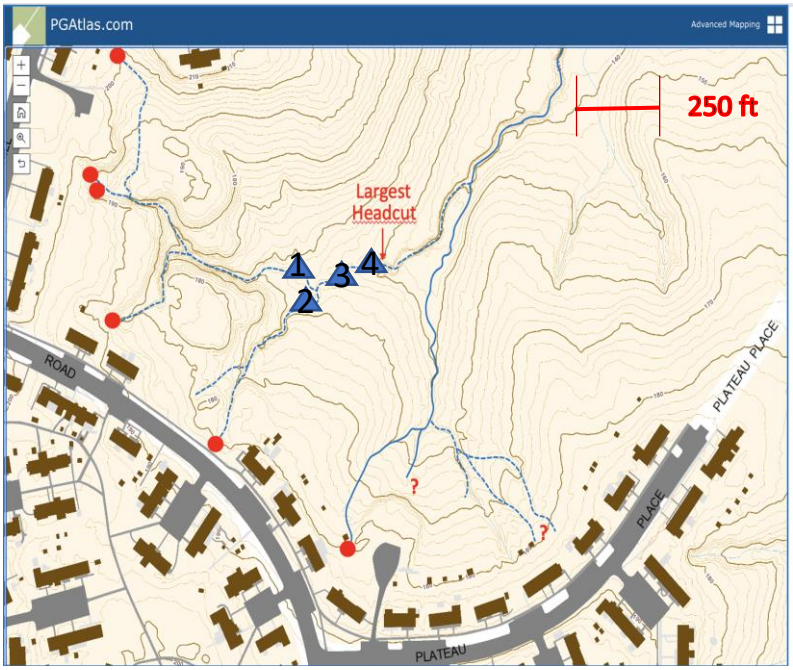

Site 1: East Tributary

Site 2: West Tributary

Site 3: Main Below Junction

Site 4: Main Near Swale

▲ Stream gauge locations

Fig 8. Flow depth gauge (Hobo) locations for each site

The water level recorders arrived on 4/20/23. I measured the recorded flow depth (obtained from scour lines and eroded leaves) at several locations along the channel axis after a major (2.6 cm) storm event prior to the arrival date to obtain water depth data. Data obtained from Stream Water Recorders were used to determine the relationship between storm precipitation amount and flow depth at various points along the length of the stream.

On 3/26/23, I measured bank-full channel characteristics, including flow depth, and flow width at 4 sites along the stream where flow depths and widths were visible after the 3/24/23 – 3/25/23 storm event. From April through October, flow depth measurements provided by the Hobo water loggers that generated data at 5-minute intervals for 4 gauge sites were acquired (Figs 21 and 24).

Calculation of Local Shear Stress During Storms:

I installed data loggers at 4 locations along the stream axis. The stream profile was surveyed with surveying equipment to determine local gradients and the relative elevation of each data logger. For each monitored storm event, flow depth from the loggers has been used in the calculation of shear stress. Peak flow depth at each station for each storm has been recorded along with the total rainfall amount. Peak shear stress for each storm event at each stream monitoring station have been determined by using the measured local gradient and depth values in the shear stress equation.

Relationships between rainfall amount and monitoring site flow depth were constructed and field evidence for channel erosion or deposition was monitored. These relationships and observations were used to determine threshold shear stresses for erosion and/or deposition at each monitoring site.

Shear stress calculations were conducted for storm events and estimated for the bank-full channel at all 4 gauge sites. Depth from gauge measurements were combined with field surveys of channel gradient to determine temporal variations in shear stress.

Results:

Infiltration Rate in the Swale:

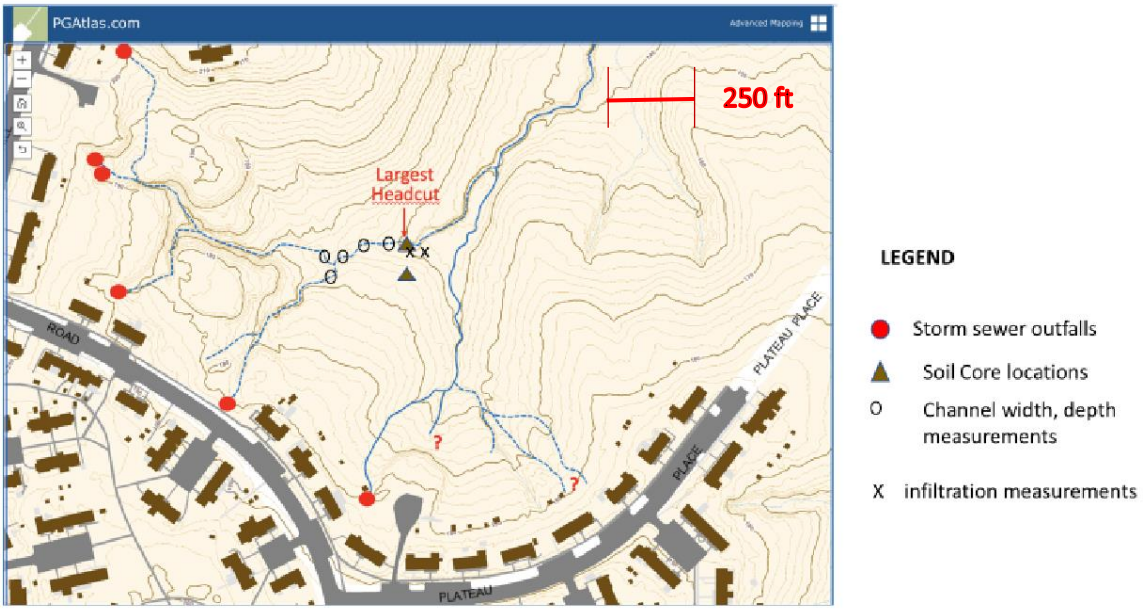

Fig 9. Location of infiltration measurements and soil cores taken on 3/26/23.

Infiltration was measured at 2 locations in the swale above the head-cut. Fig 9 shows site 1 through 6 infiltration measurement locations in increasing order from right to left starting from the largest head-cut.

Fig 10 Shows infiltration rate (cm/hr) over elapsed time (hr) for site 1 over the course of an approximated 1.05 hours. Data was obtained by calculating the change of water level in an enclosed space over time. Line of best fit (dotted line) is exponential instead of linear due to a higher R^2 value and lack of negative/zero infiltration rate values present in the data.

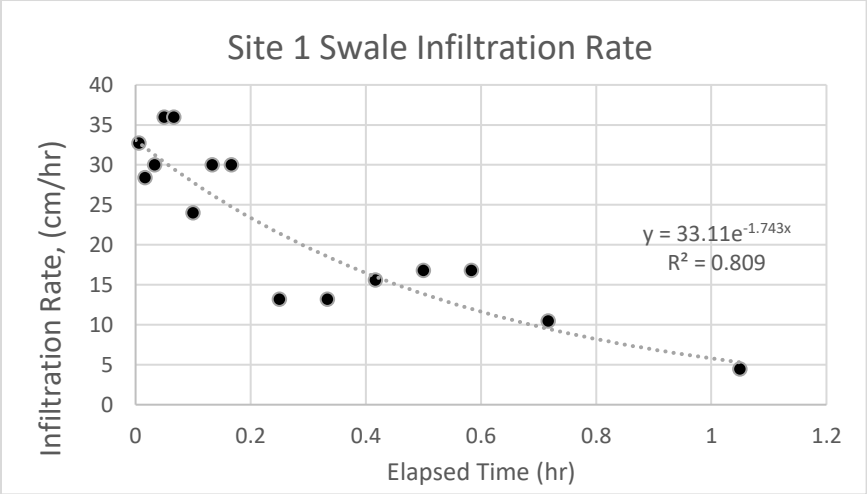

Fig 10. Rate of infiltration (cm/hr) measured over time (hr) at site 1.

The following graphs show cumulative infiltration (cm) over time (hr) for site 1 and 2 over the course of an approximated 1.05 hours (Figs 11 and 12). Data was obtained by calculating the total amount of infiltrated water seeping into the soil site over time using a body of water in an open top structure and a stopwatch. Cumulative infiltration data indicates 2 main phases of infiltration, with the second likely representing the infiltration capacity (downward movement of the wetting front).

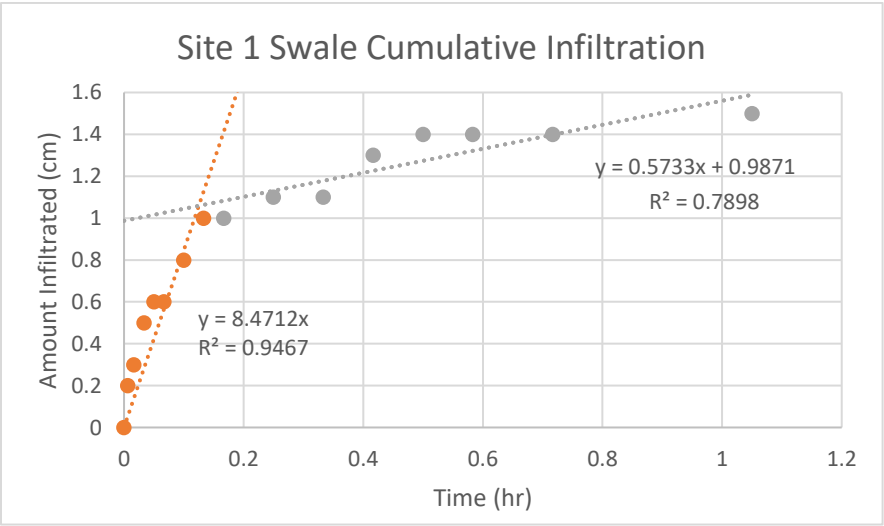

Fig 11. Cumulative infiltration (cm) measured over time (hr) at site 1

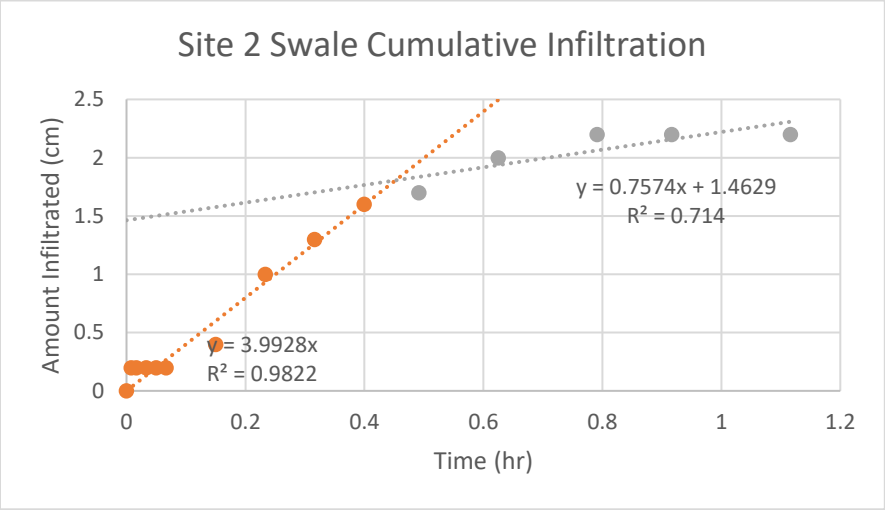

Fig 12. Cumulative infiltration (cm) measured over time (hr) at site 2.

Looking at both cumulative infiltration graphs, the infiltration rates decrease significantly after the first 10-25 minutes and provide information about the infiltration capacity in the second part of these curves.

The following table directly below (Table I) represents average infiltration rate and infiltration capacity for Swale sites 1 and 2. The average infiltration capacity of the swale site is an approximated 0.67 cm/hr.

Table I: Measured Infiltration Rates:

Site	Initial rate	Initial duration	Total infiltrated	Capacity rate
Swale 1	8.5 cm/hr	8 minutes	1.0 cm	0.57 cm/hr
Swale 2	4.0 cm/hr	24 minutes	1.55 cm	0.76 cm/hr
Ave capacity				**0.67 cm/hr**

Soil Core Measurements:

Core samples were taken from 3 locations: a) the topographic swale above the head-cut, b) the steep forested hillslope near the valley axis, and c) a dormant gully at Greenbelt National Park. These samples were obtained for their soil O horizons and soil A horizons. They were brought to the lab, each sample was weighed, air dried, and then oven dried for 13 hours at 60^{o}C. From these data, I determined water content and bulk density. Percent soil organic matter was estimated from bulk density measurements obtained from forested soils developed on Patuxent formation sedimentary formations (Volz et al, 2022). The equation that describes this relationship is:

$$\%\text{SOM (by weight)} = 3.8501(\text{Bulk Density})^{-0.833}$$

Fig 13: Core Samples of Soil O Horizons

Table II: Soil Characteristics of swale, hillslope, and reference "fossil" gully

Site	Core depth Interval from surface, cm	% Water (by weight)	Dry bulk density, g/cc	% SOM (by weight)
Hillslope above swale	0.00 – 14.0	33.25	1.09	3.58
Hillslope above swale	14.0 – 28.0	25.71	2.09	2.08
Swale above head-cut	0.00 - 11.5	28.42	1.48	2.78
Swale above head-cut	11.5 – 23.0	25.16	1.65	2.08
Fossil gully	0.00 – 13.0	51.69	0.29	10.87
Fossil gully	13.0 – 18.0	35.97	1.16	3.39

The soil samples were collected immediately the day after a storm event, so the soil was still wet. The amount of water in the soil was due to soil pore space and the absorption of water by soil organic matter. The water content, which represents water held in shallow soils, increased with lower values of soil bulk density, as shown in Fig 14.

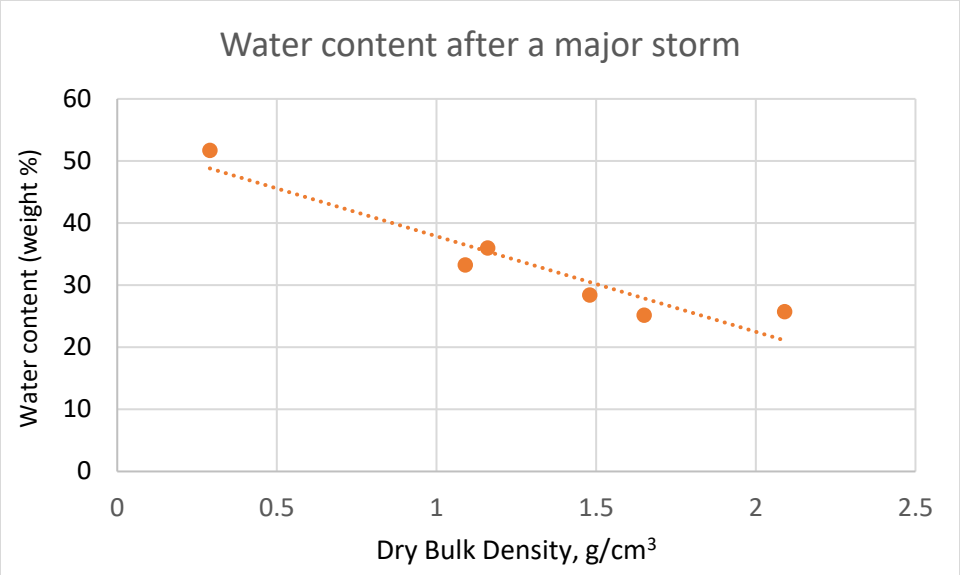

Fig 14: Relationship of water content to soil bulk density.

Field data on flow depths in the gully and on the swale above the head-cut were collected after a major storm that occurred on 3/24/23. Channel cross section measurements were conducted on 3/26/23 at six locations. Depth of flow was evident from clear erosion lines that separated cleared areas from heavy cover of leaf litter. The following table represents topographic data for the channel measurement sites 1-6. Data was collected using in-person observations and measurement devices.

Table III: Cross sections and Depth of Flow Along Channel after a 2.2 cm Storm (3/24/23)

Site #	Upstream distance from head-cut (m)	Width (m)	Maximum depth (cm)	Average depth (cm)	Minimum depth (cm)	Material
1	8.23	1.37	20.3	17.0	12.7	Soil
2	14.94	1.67	21.6	15.9	10.16	Soil, gravel, undercut
3	26.37	1.31	30.5	26.3	22.86	Soil
4	37.95	1.52	35.6	34.6	30.48	Gravel
5	42.51	0.40	15.3	15.3	15.3	Soil
6	44.04	0.86	10.7	7.1	7.1	Soil

The channel measurements indicate that the channel widens significantly as the tributaries join and the flow spreads out in the swale. The flow depth below where the tributaries join is more than 2x the flow depth of the tributaries upstream of the junction. Flow depth decreases downstream towards the head-cut as the width expands. These data,

represented in Figs 15 and 16, suggest that the flow width expansion might be the important parameter that decreases flow depth above the head-cut.

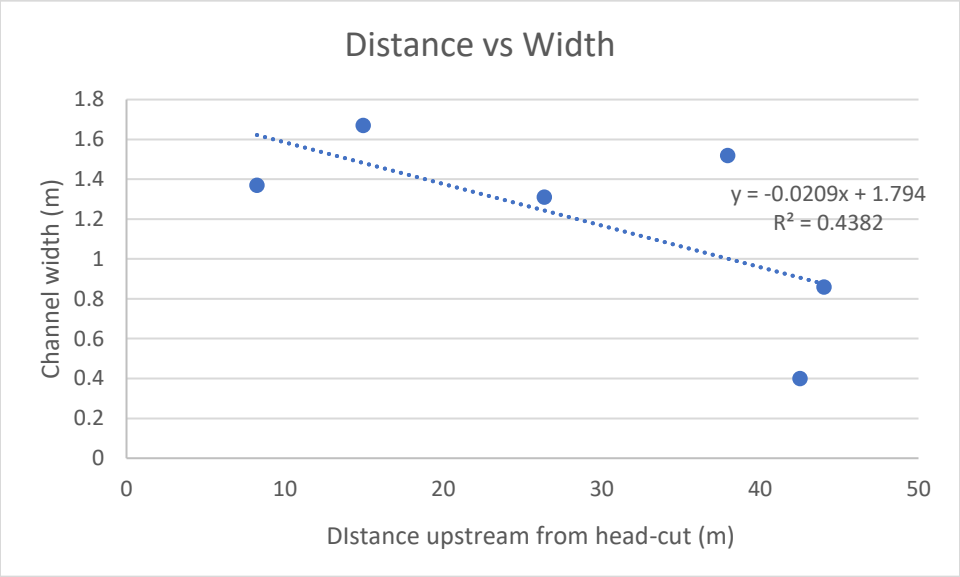

Fig 15. This graph represents Distance upstream from head-cut (m) vs measured channel width (m) with a linear trendline to determine average values and a line of best fit.

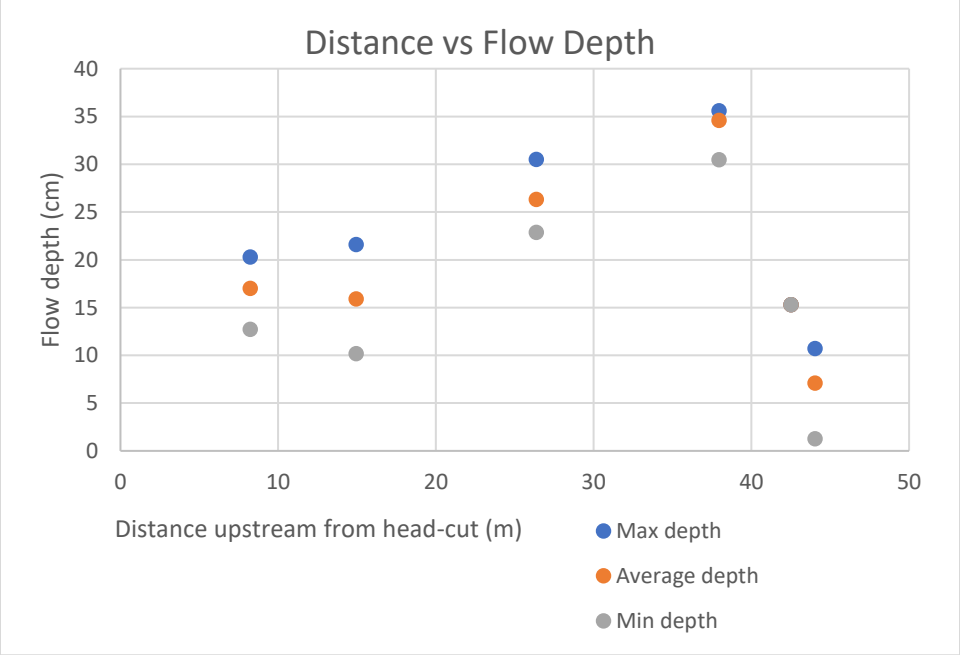

Fig 16. This graph displays distance upstream from head-cut (m) vs measured flow depth (cm) with blue, orange, and grey dots representing max, average, and minimum depths at each site respectively.

Table IV: Average and Maximum Shear Stress for 3/24/23 event

Site #	Upstream distance from head-cut (m)	Max Depth (cm)	Average depth (cm)	Slope	Max t, (N/m^2)	Average t, (N/m^2)
1	8.23	20.3	17	0.028	5.6	4.7
2	14.94	21.6	15.9	0.028	5.9	4.4
3	26.37	30.5	26.3	0.028	8.4	7.2
4	37.95	35.6	34.6	0.06	20.9	20.3
5	42.51	15.3	15.3	0.108	16.2	16.2
6	44.04	10.7	7.1	0.108	11.3	7.5

Using the gradient estimates from the longitudinal stream profile, shear stress values for the 2.6 cm 3/24/23 – 3/25/23 storm event were determined (Fig 17). Shear stress values were highest within the two tributary channels and the combined segment of the main channel below where the tributaries joined together. Both the gradient and the flow depth contribute to the high shear stress values below the junction. Although flow depth values are lower in the two tributaries, the steep gradient maintains high shear stress values. Field observations suggest erosion, and not deposition, occurred at all locations with this significant storm event. It is possible that deposition might occur at sites above the head-cut during smaller or less intense storm events.

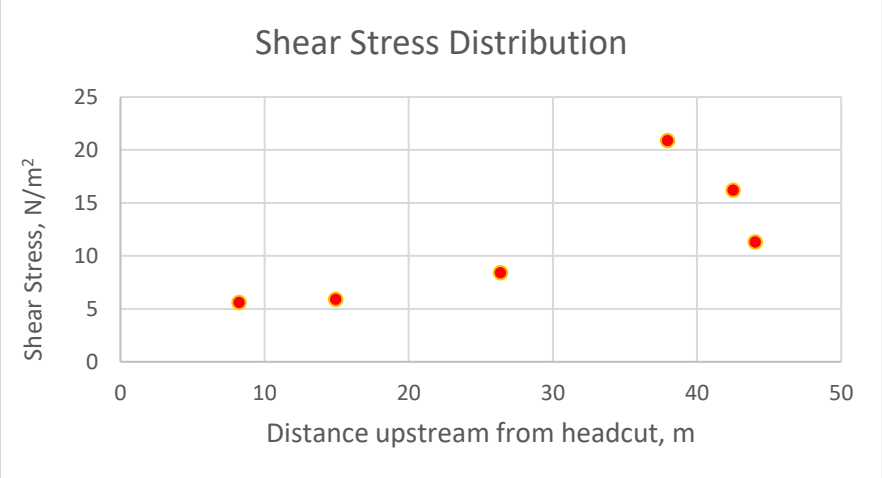

Fig 17. Distribution of Shear Stress along the channel after 3/24/23 - 3/25/23 Storm Event

Cross Section Measurements and Calculations

Cross section measurements were taken at each gauge site on 8/6/23. Measurements were then input into graphical format for visual interpretation (Fig 18). Going from upstream to downstream, Sites East Tributary, West Tributary, and Main Below Junction appear to increase

in both depth and width further downstream while site Main Near Swale stays relatively similar width wise while reducing in depth.

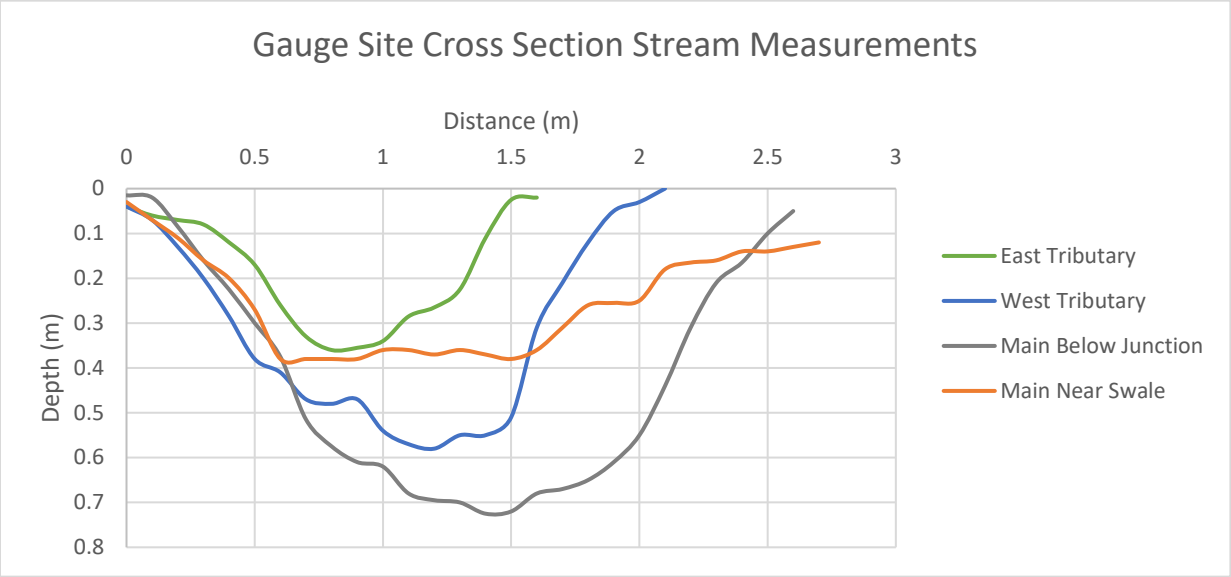

Fig 18. All 4 gauge sites cross section measurements taken on 8/6/23

To develop relationships between cross sectional area and gauge height, for use in future discharge estimates, a MATLAB script provided by Alex Lastner was used to fit graphical data. See Appendix D for Gauge Height vs Area Graphs.

Precipitation data Measurements for 4/23/23 – 5/7/23 Storm Events

Precipitation data for the period of study from 4/23/23 – 5/7/23 (Fig 19) was collected from a local Greenbelt weather gauge monitored by a community member a short distance from the study site. A zoomed in version of the 1st major storm event is plotted in Fig 20.

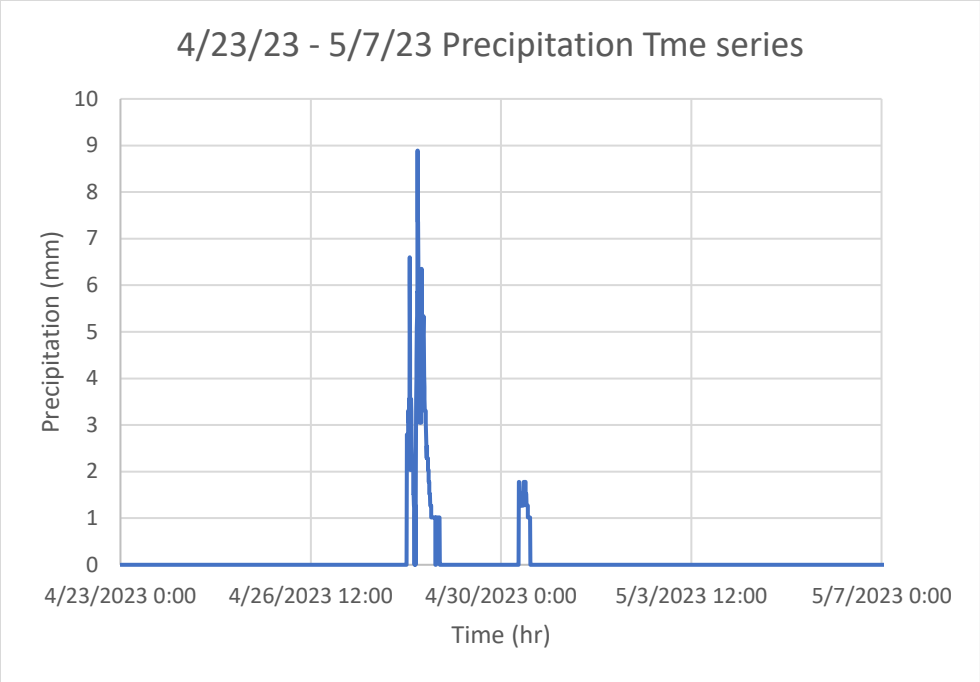

Fig 19. Precipitation for 5 min intervals for N. Greenbelt MD area from 4/23/23 – 5/7/23

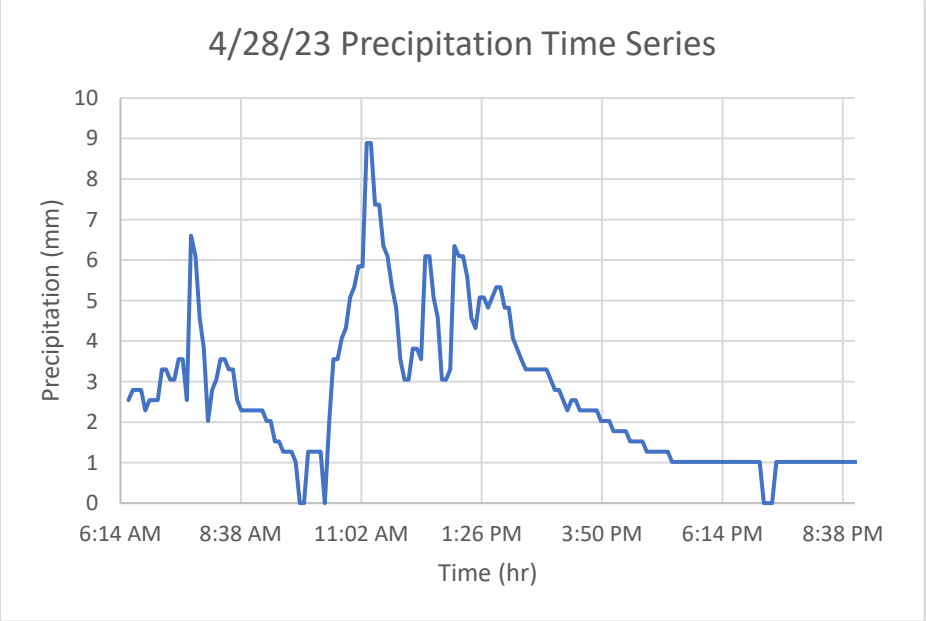

Fig 20. Precipitation for 5 min intervals for a major storm event in Greenbelt MD 4/28/23 (From Fig 19 zoomed in for clarity)

Flow Depth Measurements for 4/23/23 – 5/7/23 Storm Events

Flow depth from field evidence was measured with Hobo data loggers provided from West Tributary, Main Near Swale, and Main Below Junction gauge sites between 4/23/23 – 5/7/23. Measurements were then analyzed and graphically formatted together for visual interpretation (Fig 21). Flow Depth measurements appear to be the highest for all 3 gauge sites during each storm event. All 3 gauge sites are similar in value pre-storm. During storms, West Tributary increases in value at height of each storm event but maintains overall value consistent throughout timeframe. Main Near Swale also increases during both storm events but has significantly greater increase in value during 2nd storm event. Post-storms, values follow the negative slope into negative values. Main Below Junction follows a similar trend to Main Near Swale but instead has higher flow depth values during 1st storm rather than second. Also, post storm flow depth does not have as a significant drop in value as Main Near Swale.

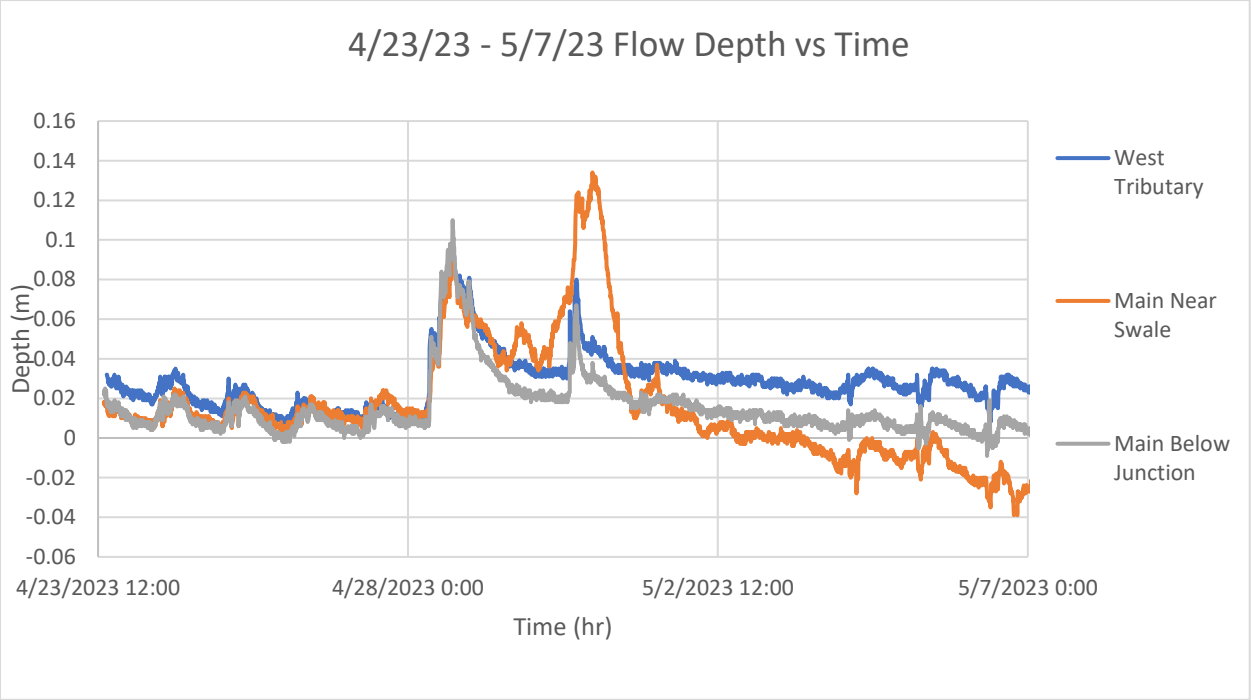

Fig 21. Flow Depth measurements of West Tributary, Main Near Swale, and Main Below Junction gauge sites over 4/23/23 – 5/7/23 timeframe.

Shear Stress Calculations for 4/23/23 - 5/7/23 Storm Events

Using the gradient estimates from the stream gradient profile (Fig 7), shear stress values for the 4/23/23 – 5/7/23 storm events were determined (Fig 22). Shear stress values were relatively low before both storm events whereas they were highest during both storm events with moderate levels remaining after said storm events. West Tributary and Main Below Junction sites appear to be relatively parallel in value with similar values for each storm event while having different slopes pre-storm events. Main Near Swale appears to instead have

higher values for the smaller storm event while maintaining a downward trend in shear stress post-storm events.

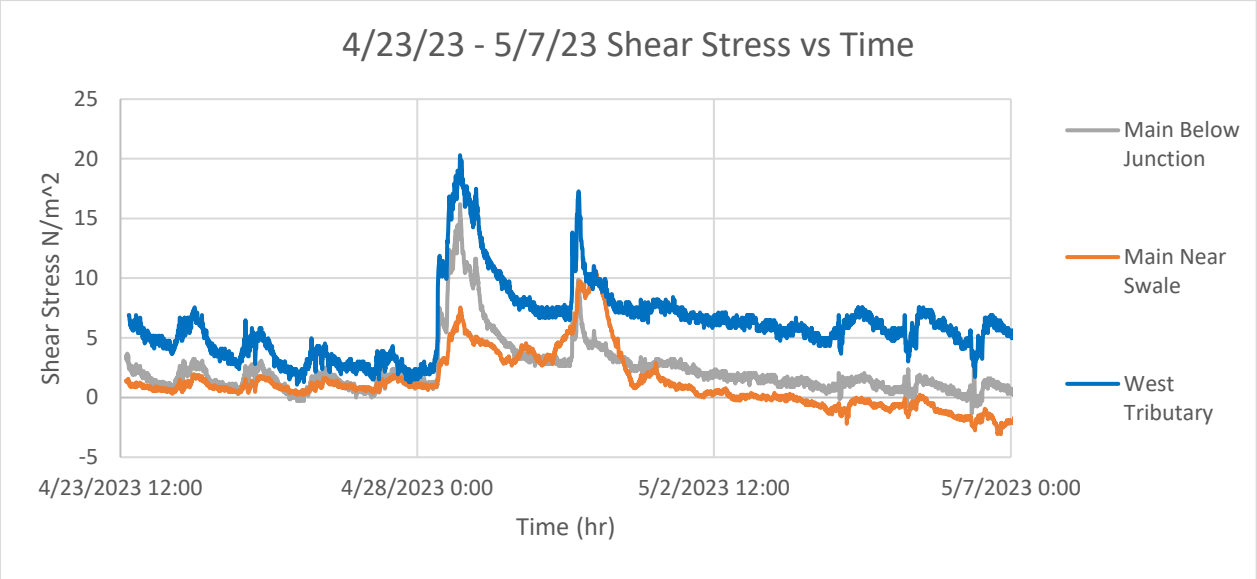

Fig 22. Distribution of Shear stress at sites West Tributary, Main Near Swale, and Main Below Junction from 4/23/23 – 5/7/23

Precipitation data Measurements for 8/6/23 – 10/19/23 Storm Events

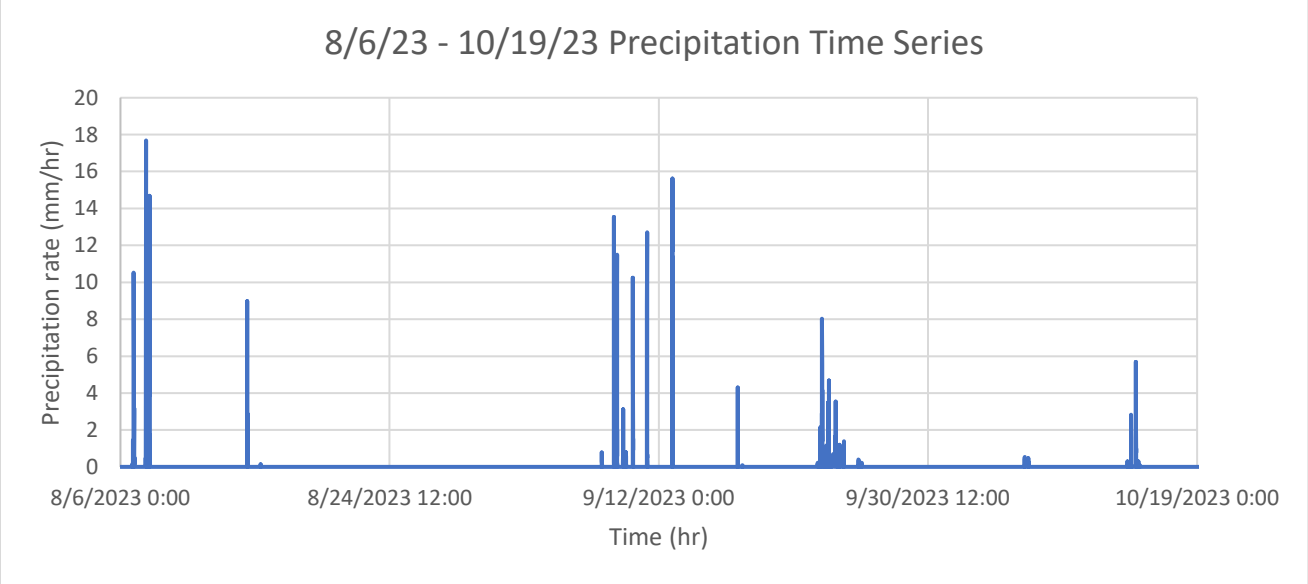

Fig 23. Precipitation measured in 5 min intervals for N. Greenbelt MD area from 8/6/23 – 10/21/23

Flow Depth Measurements for 8/6/23 – 10/19/23 Storm Events

Flow depth measurements from the field collected using Hobo data loggers were provided from all 4 gauge sites between 8/6/23 – 10/19/23. Measurements were then combined to be analyzed and graphically formatted for visual interpretation (Fig 24). Flow depth measurements display longer flow recessions during the second half of the timeframe indicating reduced available flow storage capacity over time from August. Main Below Junction, East Tributary, and West Tributary sites appear to have positive flow depth values while site Main Near Swale appears to display a low flow depth in comparison.

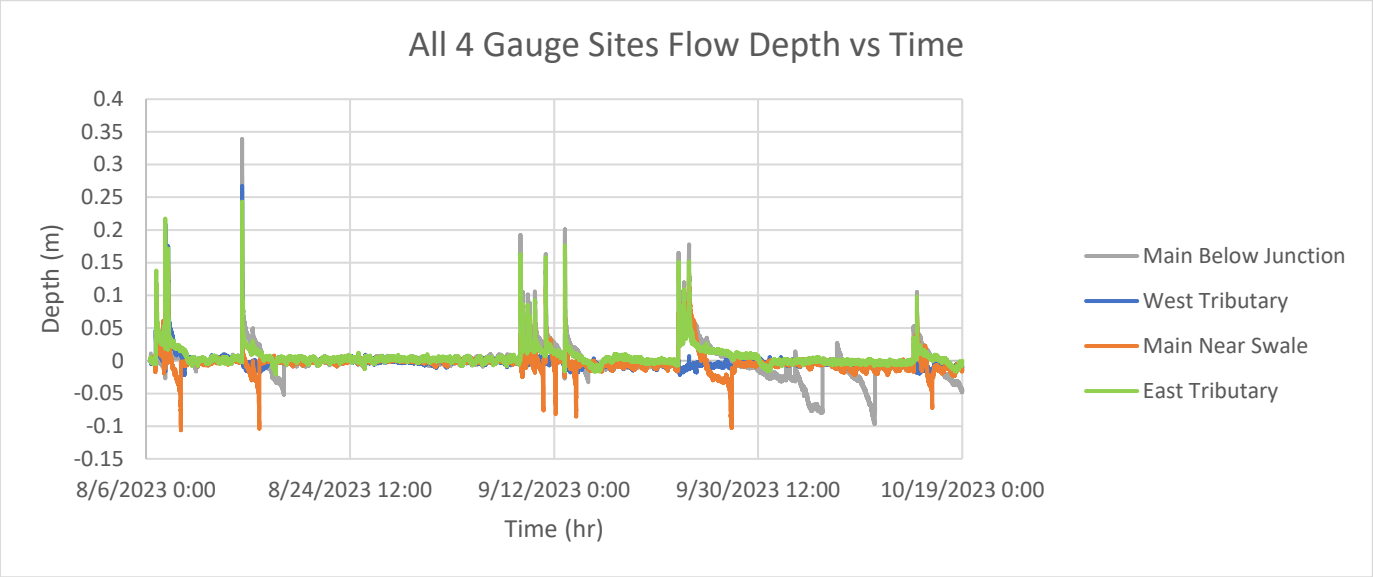

Fig 24. Flow Depth measurements of all 4 gauge sites over 8/6/23 – 10/19/23 timeframe.

Shear Stress Calculations for 8/6/23 – 10/19/23 Storm Events

Using the gradient estimates from the stream gradient profile (Fig 7), shear stress values for the 8/6/23 – 10/19/23 storm events were determined (Fig 25). Shear stress values appear to be short lived during the first half of the timeframe with near zero values apparent throughout most of late August. Mid-September, values increase with longer duration in both length of shear stress events and overall number of high stress values over time during said events in contrast with the early August events that are high in value but short-lived and sparse. This indicates increased erosion at said locations after their respective storm events during September because of increased shear stress and flow combined with a presumed low storage capacity due to extended recession events following said storm events.

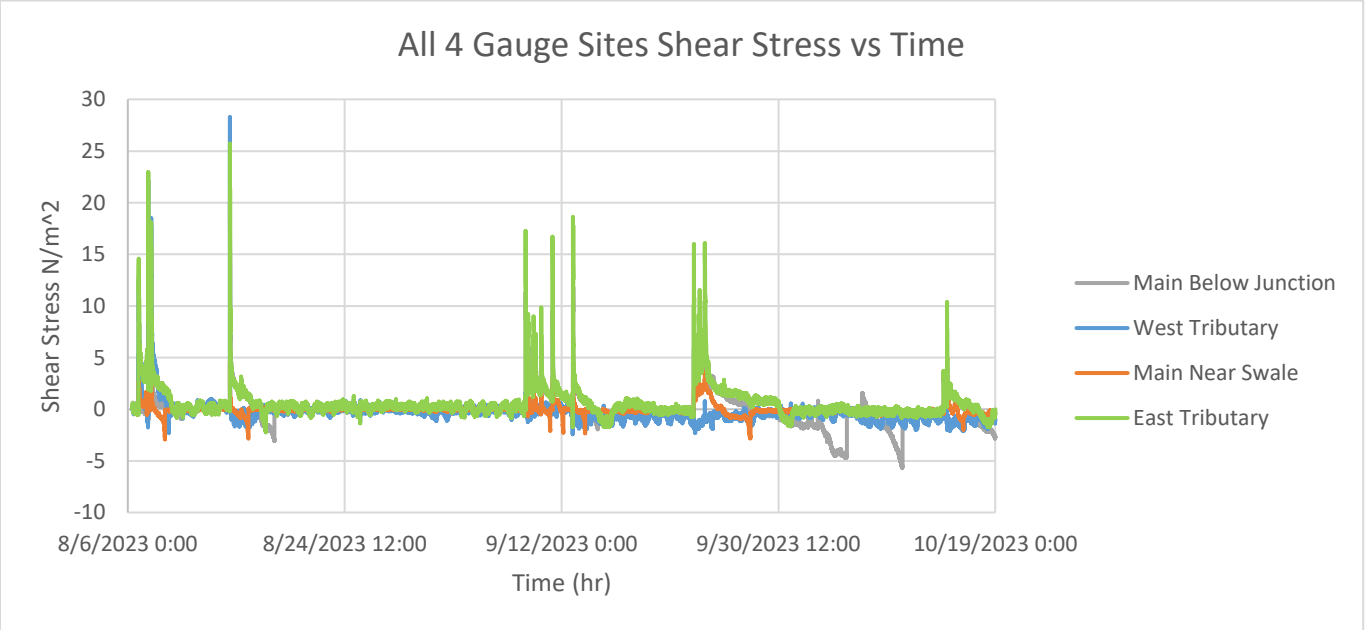

Fig 25. Distribution of Shear stress along the channel 8/6/23 – 10/19/23

Grain Diameter Measurements and Observations:

Table V: Grain Size Diameter Distribution Along Channel

Site:	Mean Grain Diameter (mm):
East Tributary	26.0
West Tributary	29.2
Main Below Junction	31.8
Main near Swale	18.0

Mean grain diameter measurements taken on 10/22/23 at each site appear to gradually increase in overall diameter further downstream before reducing in value at site Main Near Swale. Grains are likely sourced from erosion of road gravel, possibly before roads were paved. The material could have been added to the stream to stabilize it, but this could not be documented. Gravel material is shale and limestone, not part of the underlying formation (Fig 26). See Appendix E for individual grain diameter measurements.

Fig 26. Grains used for measurement taken from Main Below Junction site displayed on log for visual reference.

Discussion and Summary:

This project was designed to evaluate erosion in a small tributary stream that receives urban runoff and conveys it downstream to an incised portion of the stream. The small tributaries that receive the runoff are incised, but an unchanneled swale extends between these tributaries and the downstream massive head-cut. The community is concerned that the downstream head-cut will propagate upstream.

To evaluate processes operating between the tributary and head-cut, I measured soil properties (infiltration capacity, soil bulk density, and soil organic matter content) in the swale and compared them to reference sites on adjacent hillslopes and non-eroding, “fossil” gullies located in nearby non-urban watersheds. Collected data indicates that infiltration rate in the hillslope swale area demonstrated a rapidly decreasing infiltration rate over time. The average infiltration capacity for the two sites measured was 0.67 cm/hr, which is quite low for forest soils. This is consistent with the finding that the swale O horizon bulk density is higher (less porosity or organic matter) than organic horizons on the hillslope and at the reference sites. Measurements also indicate that both organic matter content and water content after a major storm were lower in the swale than on the hillslope or reference non-eroding gully site. This suggests that infiltration into the heavily trampled swale above the head-cut could be improved by diverting the trails away from the area.

Flow depths associated with a 2.2 cm 3/24/23 – 3/25/23 storm event were measured at 6 locations along the valley axis. These data sets indicate that the flow depth and shear stress was highest below the tributary junction (where the channel depth is also the deepest). The decrease in channel gradient in the channel above the head-cut (swale area) caused the flow width to expand, water depth to decrease, and the shear stress to decrease. There was evidence of recent gravel deposition between the tributary junction and unchanneled swale. events that generate shallower runoff depths might cause soil deposition in the swale location, which would keep the gradient flat.

Flow depths associated with a 4/23/23 – 5/7/23 storm event were measured at the West Tributary, Main Below Junction, and Main Near Swale gauge sites along the stream. All 3 sites displayed similar flow depth values during the first major storm event. During the second storm event, sites Main Below Junction and Main Near Swale experienced a similar increase in flow depth values. However, site Main Near Swale experienced a significantly greater flow depth value increase as opposed to the Main Below Junction and West Tributary gauge sites. After the second storm event, Main Near Swale flow depth values gradually reduced to values lower than those recorded before the first storm event. Also, Main Below Junction flow depth values remained similar to those seen before the first storm event. Lastly, West Tributary flow depth values gradually increased to greater than those seen before the first storm event. When converted to shear stress values using gradient estimates from the stream gradient profile (Fig 7), these data sets indicate that the shear stress was highest during a major storm event with the West Tributary site containing larger residual shear stress values as opposed to the Main Below Junction and Main Near Swale sites located further downstream.

Flow depths associated with the 8/6/23 – 10/19/23 storm events were measured at the East Tributary, West Tributary, Main Below Junction, and Main Near Swale gauge sites along the stream. All 4 sites displayed varying flow depth values throughout each storm event with each tributary site having greater flow depth values than the Main Below Junction and Main Near Swale sites located further downstream. Beginning mid-September, flow depth values at each site experienced longer flow recessions indicating reduced available flow storage capacity over time from first half of the timeframe. When converted to shear stress values using gradient estimates from the stream gradient profile (Fig 7), these data indicate that the shear stress calculated at each site increased significantly during a major storm event. The West Tributary demonstrated the highest shear stress values while the East Tributary site demonstrated the second highest shear stress. Gradient decreased downstream from both tributary locations, the site below the tributary Junction had the 2nd lowest shear stress values while site Main Near Swale had the lowest shear stress values.

The data collected provides quantitative support to both hypotheses regarding stream channel erosion and infiltration. Storm water runoff from nearby sewer outlets appears to be directly linked to stream channel erosion downstream from the outlets. Maximum shear stress

values decrease downstream from the tributary junction and deposition rather than erosion is occurring above the head-cut.

Acknowledgments:

The equipment for this project has been provided by the Woodland Committee of the City of Greenbelt through a small grant written by Professor Prestegaard and Catherine Plaisant. I thank Catherine Plaisant for joining us in the field, helping with field data collection and sharing her observations and photographs of the field site during storm events.

References:

ArcGIS Web Application. Geodata.md.gov. Retrieved February 28, 2023, from https://geodata.md.gov/topoviewer/

Castillo, C., & Gómez, J. A. (2016). A century of gully erosion research: Urgency, complexity and study approaches. *Earth-Science Reviews*, *160*, 300-319.

Chen, W., Huang, C., Chang, M., Chang, P., & Lu, H. (2013). The impact of floods on infiltration rates in a disconnected stream. *Water Resources Research*, *49*(12), 7887-7899.

Fanelli, R., Prestegaard, K., & Palmer, M. (2017). Evaluation of infiltration-based stormwater management to restore hydrological processes in urban headwater streams. *Hydrological Processes*, *31*(19), 3306-3319.

Glaser, J. (2003) Geological Map of Prince George's County, Maryland (And Silt-Loam Soils with Hardpan in Upland Deposits from Hack (1977)). Maryland Geological Survey. Downloaded from https://ngmdb.usgs.gov/Prodesc/proddesc_104906.htm on 4/17/2023.

Gregory, J. H., Dukes, M. D., Jones, P. H., & Miller, G. L. (2006). Effect of urban soil compaction on infiltration rate. *Journal of Soil and Water Conservation*, *61*(3), 117-124.

Leopold, L. B. (1968). *Hydrology for urban land planning: A guidebook on the hydrologic effects of urban land use* US Geological Survey Circular 554.

MacDonald, L. H., & Coe, D. (2007). Influence of headwater streams on downstream reaches in forested areas. *Forest Science*, *53*(2), 148-168.

Montgomery, D. R., & Dietrich, W. E. (1988). Where do channels begin? *Nature*, *336*(6196), 232-234.

Rose, S., & Peters, N. E. (2001). Effects of urbanization on streamflow in the Atlanta area (Georgia, USA): a comparative hydrological approach. *Hydrological processes*, *15*(8), 1441-1457.

Schwendel, A. C., Death, R. G., & Fuller, I. C. (2010). The assessment of shear stress and bed stability in stream ecology. *Freshwater Biology*, *55*(2), 261-281.

Obermeier, S. F. (1984). Engineering geology of Potomac Formation deposits in Fairfax County, Virginia and vicinity with emphasis on landslides. *Geological Survey Bulletin*, *1556*, 5-48.

Volz, S. (2020). Effects of Soil Characteristics on Evapotranspiration-Driven Water Table Decline and Recovery in a Forested Floodplain. Undergraduate University of Maryland Senior Thesis.

Volz, S. Ravi, R., & Prestegaard, K. (2022) Comparison of Above Ground and Below Ground Carbon Stocks in a Managed Suburban Landscape: GSA abstract, NE Meeting

Wynn, T. M., Mostaghimi, S., & Alphin, E. F. (2004). The effects of vegetation on stream bank erosion. In *2004 ASAE Annual Meeting* (p. 1). American Society of Agricultural and Biological Engineers

Appendix:

Appendix A: Organic Matter Calculations

Weight %SOM Graph

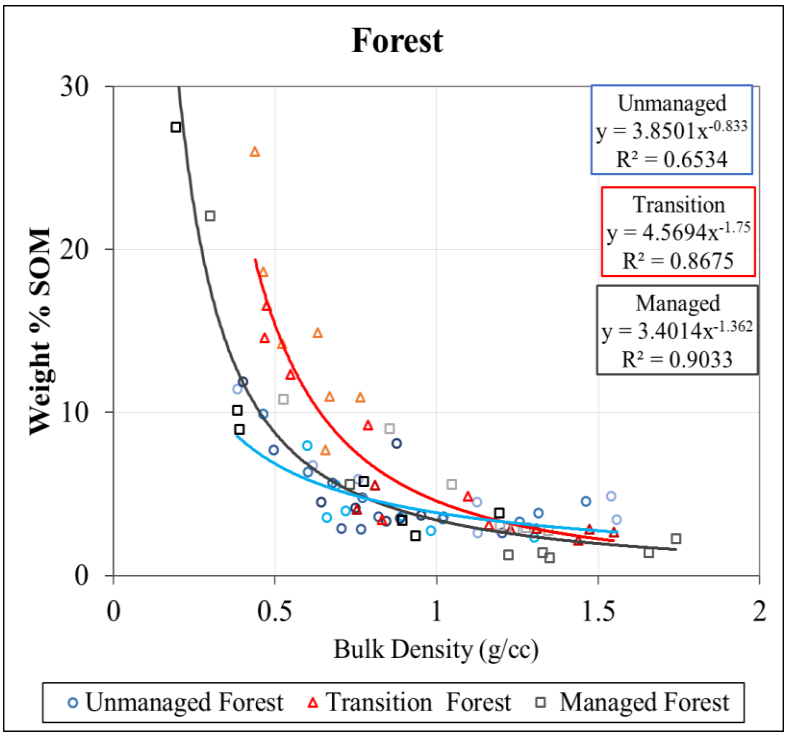

Appendix B: Bulk Density and Water Content Calculations

Wet Bulk Density Calculations:

Site	Core depth interval from surface, cm	Core volume, cm^3	Wet weight + plastic bag container (5.9g), g	Wet bulk density (without plastic bag container) g/cm^3
Hillslope above swale	14.0	212.3	353.3	1.6

Hillslope above swale	14.0 – 28.0	212.3	604.1	2.8
Swale above head-cut	11.5	173.7	364.8	2.1
Swale above head-cut	11.5 – 23.0	173.7	387.8	2.2
Fossil gully	0 – 13.0	193	120.8	0.6
Fossil gully	13.0– 18.0	77.2	146.3	1.8

Dry Bulk Density Calculations:

Site	**Core depth interval from surface, cm**	**Core volume, cm^3**	**Dry weight + plate, g**	**Plate weight, g**	**Dry bulk density (without plate weight) g/cm^3**
Hillslope above swale	14.0	212.3	409.1	177.2	1.090
Hillslope above swale	14.0 – 28.0	212.3	627.6	183.2	2.090
Swale above head-cut	11.5	173.7	431.6	174.7	1.480
Swale above head-cut	11.5 – 23.0	173.7	458.4	172.6	1.650
Fossil gully	0 – 13.0	193.0	232.4	176.9	0.290

Fossil gully	13.0– 18.0	77.20	268.2	178.3	1.160

Water Content Calculations:

Site	wet bulk density g/cm^3	dry bulk density g/cm^3	Water content ratio g/cm^3	% Water
Hillslope above swale	1.6	1.09	0.54	33
Hillslope above swale	2.8	2.09	0.72	25.7
Swale above head-cut	2.1	1.48	0.59	28.4
Swale above head-cut	2.2	1.65	0.55	25.2
Fossil gully	0.6	0.29	0.31	51.7
Fossil gully	1.8	1.16	0.65	36.0

Appendix C: Longitudinal Profile Survey Data 4/24/2023

Survey Data:

Indicator	Distance from head-cut (ft)	Distance from head-cut (m)	FS (Foresite) (m)	HI (Height of instrument) (Backsight + Elevation of benchmark (10))	HI - FS (Elevation)
Backsight				11.803	10.00

(1.803) (Gauge)					
	7	2.134	2.300	11.803	9.503
	9	2.743	2.993	11.803	8.81
	11	3.353	2.998	11.803	8.805
	13	3.962	2.312	11.803	9.491
	15	4.572	2.345	11.803	9.458
	17	5.181	2.338	11.803	9.465
	19	5.791	2.362	11.803	9.441
	21	6.400	2.39	11.803	9.413
	23	7.010	2.395	11.803	9.408
	25	7.620	2.315	11.803	9.488
	27	8.229	2.297	11.803	9.506
	29	8.839	2.25	11.803	9.553
	31	9.448	2.255	11.803	9.548
	33	10.06	2.29	11.803	9.513
	35	10.67	2.272	11.803	9.531
	37	11.28	2.302	11.803	9.501
	39	11.89	2.282	11.803	9.521
	41	12.49	2.255	11.803	9.548
	43	13.11	2.27	11.803	9.533
Gauge	45	13.72	2.26	11.803	9.543
	47	14.32	2.25	11.803	9.553
	49	14.93	2.245	11.803	9.558
	51	15.54	2.23	11.803	9.573
	53	16.15	2.24	11.803	9.563
	55	16.76	2.22	11.803	9.583
	57	17.37	2.22	11.803	9.583
	59	17.98	2.212	11.803	9.591
	61	18.59	2.182	11.803	9.621

63	19.20	2.168	11.803	9.635
65	19.81	2.135	11.803	9.668
67	20.42	2.105	11.803	9.698
69	21.03	2.107	11.803	9.696
71	21.64	2.08	11.803	9.723
73	22.25	2.06	11.803	9.743
75	22.86	2.07	11.803	9.733
77	23.47	2.108	11.803	9.695
79	24.08	2.145	11.803	9.658
81	24.69	2.142	11.803	9.661
83	25.30	2.182	11.803	9.621
85	25.90	2.183	11.803	9.62
89	27.12	2.157	11.803	9.646
91	27.73	2.2	11.803	9.603
93	28.34	2.05	11.803	9.753
95	28.95	2.042	11.803	9.761
97	29.56	2.02	11.803	9.783
99	30.17	2.032	11.803	9.771
101	30.78	2.05	11.803	9.753
103	31.39	2.082	11.803	9.721
105	32.00	2.092	11.803	9.711
107	32.61	2.091	11.803	9.712
109	33.22	2.135	11.803	9.668
111	33.83	2.13	11.803	9.673

Appendix D: Gauge Height vs Area Graphs:

Gauge Height vs Area Graphs:

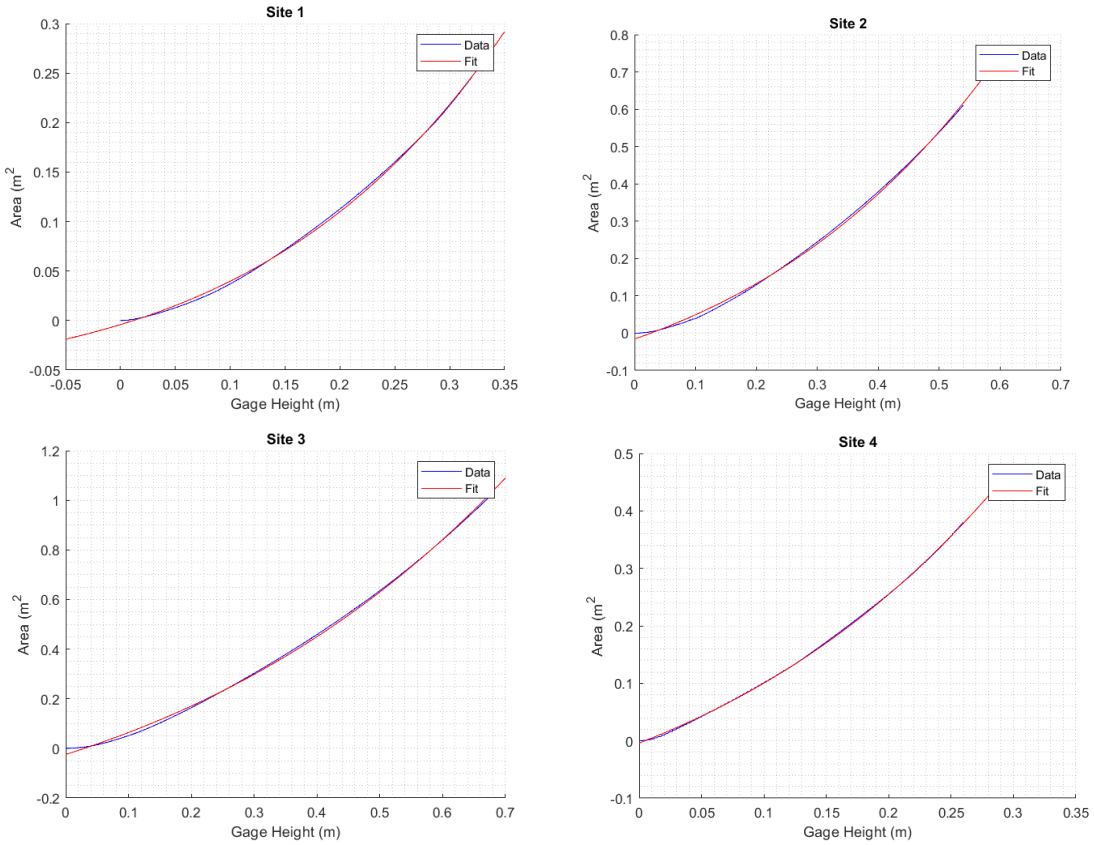

(Top left) Site 1 East Tributary Gauge Height vs Area. (Top right) Site 2 West Tributary Gauge Height vs Area. (Bottom left) Site 3 Main Below Junction Gauge Height vs Area. (Bottom right) Site 4 Main Near Swale Gauge Height vs Area

Appendix E: Grain Diameter Measurements

Grain Diameter Measurements:

Site:	Grain 1 (mm)	Grain 2 (mm)	Grain 3 (mm)	Grain 4 (mm)	Grain 5 (mm)	Grain 6 (mm)	Grain 7 (mm)	Grain 8 (mm)	Grain 9 (mm)	Grain 10 (mm)	Mean Average (mm)
Main Below Junction	29	30	35	49	36	31	29	26	19	34	31.8
West Tributary	26	31	24	34	25	35					29.2

East Tributary	23	19	34	30	29	23	24	26		26
Main Near Swale	16	18	17	19	20					18

DEPARTMENT OF
GEOLOGY

Honor Pledge/Statement

I pledge on my honor that I have not given or received any unauthorized assistance on this assignment or examination.